Rheol Acta (2003) 42: 516–526
DOI 10.1007/s00397-003-0306-y

ORIGINAL CONTRIBUTION

**Simon J. Haward**
**Jeffrey A. Odell**

# Viscosity enhancement In non-Newtonian flow of dilute polymer solutions through crystallographic porous media

Received: 28 October 2002
Accepted: 28 February 2002
Published online: 13 May 2003


S.J. Haward · J.A. Odell (✉)
H.H. Wills Physics Dept.,
University of Bristol,
Tyndall Avenue, Bristol, BS8 1TL, UK
E-mail: jeff.odell@bristol.ac.uk

**Abstract** We report results of the flow of dilute mono-disperse solutions of atactic poly(styrene) in dioctyl phthalate through regular crystallographic packed beds of spheres. Pressure drop measurements made as a function of flow rate across simple cubic and body centred cubic arrays of spheres have been used to estimate the specific viscosities of the polymer solutions as a function of the superficial Deborah number. Through both structures the onset Deborah number for the non-Newtonian increase in specific viscosity is found to be low when compared on the basis of well-characterized Zimm relaxation times. Surprisingly it is found that polymer solutions achieve a greater maximum specific viscosity in the simple cubic than in the body centred cubic array, a result contrary to prior expectations due to the absence of trailing stagnation points in the simple cubic structure. It is hypothesised that the trailing stagnation points in the body centred cubic array may be screened from the flow field by strands of oriented polymer and that, as such, the periodic variations in cross-sectional area of the flow (which are more severe in the simple cubic array) may play the most significant role in causing polymer extension and in enhancing the non-Newtonian viscosity.

**Keywords** Porous media · Extensional flow · Polymer solution · Crystallographic

## Introduction

In many practical flow situations solutions of flexible polymers are found to exhibit a well-known non-Newtonian viscosity enhancement effect. This is likely to be due to extensional components in the flow field, which can cause flexible polymer molecules to stretch and orientate, causing an increase in the extensional viscosity. This viscosity enhancement is important in many industrial applications, including food technology, paint and cosmetic formulation and enhanced oil recovery (EOR).

Potential EOR applications based upon polymer solution flooding depend upon studies of porous media flow of polymer solutions in order to optimise the use of polymers as additives in the solutions used for oilfield flooding. One essential ingredient is the achievement of effective viscosity matching at the oil-solution interface. Remarkably, this can be achieved with low concentrations of ultra-high molecular weight polymers in water or brine. However the large viscosity enhancement that occurs when polymer solutions flow through porous media, which can be exploited for EOR, is not well understood, mainly due to difficulties defining the complex random geometry of the flow field and probing the molecular response of the polymers within the porous medium.

Porous media are usually modelled experimentally by randomly packed beds of spheres. The flow of

polymer solutions around single isolated spheres is a complex problem itself and one that needs to be understood properly if the results of porous media flow experiments are to be correctly interpreted. It is known that spheres and particles experience significant non-Newtonian increases in drag when falling through polymer solutions and this is likely to be related to the viscosity increase in porous media. It is also known that at sufficient flow velocities the trailing stagnation point of a sphere can create a significant extensional flow field, strong enough to orient flexible polymers (Haward and Odell 2003).

In another publication we have addressed some of the issues associated with the flow of dilute mono-disperse atactic poly(styrene) (a-PS) solutions around spheres (Haward and Odell 2003). In the current article we present results obtained from the flow of the same solutions through porous media constructed from crystallographic arrays of spheres. Simple cubic (SC) and body centred cubic (BCC) porous media were made to simplify and idealize the flow geometry of the problem while remaining in the three-dimensional regime. The geometries of the two porous media differed greatly. With flow along the cube sides, the SC array contained no trailing stagnation points in the orientation of the flow axis, while the BCC array contained one trailing stagnation point for each sphere in the bulk of the array. Flow resistance measurements were made across the regular porous arrays to help discern the relative significance of trailing stagnation points, and other possible contributors to the extensional flow field (i.e. variations in the cross-sectional area of the flow), to the viscosification process.

## Background

There is a large body of literature on porous media flow of polymer solutions. One of the most interesting and studied aspects of the flow of polymer solutions through porous media is the non-Newtonian increase in flow resistance, which occurs for flexible polymers when a critical flow rate is exceeded. Among the first to observe this effect using randomly packed beds of spheres were Dauben and Menzie (1967) and Marshall and Metzner (1967).

James and McLaren (1975) with dilute aqueous solutions of poly(ethylene oxide) (PEO) concluded that an increase in the extensional viscosity of the polymer solution in the pore-spaces is essential to explain the critical increase in flow resistance, an opinion supported by the results of Durst et al. (1981) and Kulicke and Haas (1984).

In porous media modelled by randomly packed beds of spheres there exists a highly complex random flow geometry consisting of successive, ''pseudo-periodic'', expansions and contractions between the connected pores and many trailing stagnation points. The understanding of the stagnation point flow around spheres is vital to the understanding of porous media flow at the particle level. In flow around a single sphere the trailing stagnation point has been found to be the dominant region for producing non-Newtonian increases in extensional viscosity and molecular orientation (Haward and Odell 2003). The effect of the wake of one sphere upon a following sphere (i.e. the ''velocity effect'') has important implications regarding the mechanism by which interactions may occur between the particles that form a porous matrix (Haward and Odell 2003).

Such effects associated with stagnation point flows of highly dilute solutions have led to the suggestion that the origin of the pronounced non-Newtonian dilatancy arises from a coil↔stretch transition in polymer dynamics. Such transitions were first postulated by de Gennes (1974) and Hinch (1977) who suggested that, in an extensional flow, if the strain rate exceeds the reciprocal of the polymer relaxation time (Deborah number, $De$, $\geq\sim 0.5$) then the coil will begin to unravel. de Gennes further suggested that the unravelling process could be critical in strain rate due to a change in the draining characteristics of the coils from non-free draining to free draining (or the change in the hydrodynamic interaction between the polymer segments and solvent) as extension proceeds. This would lead to a hysteresis in the coil↔stretch process.

In order to extend substantially high molecular weight flexible polymers from the random coil, a very high accumulated strain ($\epsilon\sim 100$) is required, where

$$\varepsilon = \frac{L_o}{\langle r_o^2 \rangle^{1/2}} \tag{1}$$

where $L_o$ is the chain extended length and $r_o$ is the equilibrium end-to-end distance. This introduces a second condition for the coil↔stretch process to produce pronounced non-Newtonian effects: the extensional flow must persist long enough to stretch the molecules. The fluid strain must, therefore, be at least as great as the strain required to stretch the molecules. In fact at modest Deborah numbers the molecules will not extend affinely with the fluid elements in which they sit and much greater fluid strains are required. The realization of this latter condition is most effectively achieved around stagnation point singularities, where the strain-rate is finite, but the residence time, and therefore the fluid strain is infinite.

This model of the dilute solution coil↔stretch process has been well-supported by experimental work in idealised flows, where stagnation points give rise to narrow strands of highly extended molecules of high local extensional viscosity (Miles and Keller 1980; Keller and Odell 1985). The narrowness is due directly to the

requirement for high fluid strains, which occur only along streamlines that pass very close to the stagnation point.

A strong, though transient, extensional component will arise in a flow field without the presence of a trailing stagnation point when there is a sudden large contraction or expansion in the cross sectional area of the flow, see e.g. Cogswell (1978) and James and Saringer (1980), who examine sink flows. Cressely and Hocquart (1981) with aqueous solutions of poly(ethylene oxide) (PEO, $M_w = 4\times10^6$) at concentrations as low as 0.008%, have demonstrated that dilute polymer solutions can accumulate large strains without the presence of a trailing stagnation point by the observation of birefringent lines in an oscillatory convergent/divergent flow cell. Dyakonova et al. (1996) have performed the same experiment with dilute solutions of a-PS in tricresylphosphate (a-PS in TCP).

Also with dilute solutions of a-PS in TCP, Dyakonova et al. (1996) have shown that significant increases in the birefringence and flow resistance can occur in a cylinder array cell without a trailing stagnation point. This result suggests that symmetric periodic flows can produce accumulating strains, even though the fluid stain in an individual ''pore'' is very modest (of order 5).

This is a feature generally not seen in FENE or Brownian dumbbell modelling, where symmetric cyclic flows do not accumulate strain; the dumbbells simply contract back to the original dimensions on exiting the pore. It has been postulated that incorporation of the de Gennes hysteresis might explain strain accumulation but most studies have not found this. Some recent modelling using a Chilcott-Rallinson model (Chilcott and Rallinson 1988) incorporating hysteresis in the hydrodynamic interaction has reported accumulating strains over a limited range of Deborah number and highly dependent upon the initial boundary conditions (Odell and Carrington 2001).

Dyakonova et al. also found that when a trailing stagnation point was introduced into the cell both the birefringence and the flow resistance increased more rapidly and to greater maximum values (Dyakonova et al. 1996) illustrating the importance of the trailing stagnation point in producing large deviations from Newtonian flow behaviour, which in turn suggests the importance of polymer extension and orientation to the viscosification process.

A study of the flow of ultra high molecular weight poly(acrylamide) solutions ($M_w = 18.2\times10^6$ in ethylene glycol) through regularly packed beds has been undertaken previously by Haas and Durst (1982). Orthorhombic and cubic arrangements of spheres were constructed. However, it should be noted that neither arrangement presented trailing stagnation points in the flow direction. The authors noted that the strain in a given ''pore'' was small ($\sim$5 for the cubic cell). The specific flow resistance was measured as a function of flow-rate for different numbers of repeat unit cells, finding a progressive increase over the passage of fluid through up to four unit cells, followed by a reduction for further repeats. The authors speculated that the molecular strain must increase as fluid elements pass from one pore to the next. The reduction in resistance coefficient for passage through more than four pores is likely due to extensional thermo-mechanical degradation of the ultra-high molecular weight polymers.

The authors attempted to define the critical Deborah number corresponding to the flow rates at the onset of the increase in flow resistance from Zimm relaxation times calculated for the poly(acrylamide) system. They derived a numerical factor for each geometry to relate the observed superficial Deborah number to that derived from the calculated Zimm relaxation time. They observed that the unscaled Deborah numbers were much lower than the expected value of $\sim$0.5

Interestingly, the flow resistance in a randomly packed bed was equivalent to a linear superposition of the flow resistance through the two regularly packed beds. The authors explained this by the observation that a random arrangement of spheres can be thought of as a random superposition of regular unit cells. However, the result remains surprising since neither of the regularly packed beds contained any trailing stagnation points, which must necessarily be present in any random packing of spheres.

Saez et al. (1994) reported observations of non-Newtonian extensional flow effects coupled with birefringence in porous media flow of mono-disperse atactic poly(styrene) solutions, $M_p = 12.25\times10^6$, $c = 0.08\%$, well below the conventional overlap concentration $c^*$. The authors argued that the non-Newtonian effects observed in porous media flow are best explained by the formation of transient networks of entangled molecules, a theory first proposed by Odell et al. (1988) to account for the highly critical nature of the viscosity increases observed with poly-disperse polymer solutions.

Muller et al. (1998) performed flow visualization experiments on a randomly packed porous media with a 0.1% solution of poly(alphaolefine) in paraffin oil by matching the refractive index of the solution to that of the porous media. Above a critical flow rate the polymer solution displayed a pronounced non-uniform flow pattern and showed a preference to flow only along certain narrow paths through the porous media. The preferred paths were found to fluctuate over a timescale of the order of 2 s. The authors concluded that the increase in extensional viscosity when the polymers stretch leads to irregularities in the flow field, which in turn cause the flow resistance to increase. It should be noted that these experiments were in random porous media, so it might be anticipated that local high values of strain-rate would lead to local stretching.

For an extensive review of work on porous media flow see Muller and Saez (1999).

In the present study we report results from the flow of solutions of well characterized, highly dilute, monodisperse a-PS in di-octyl phthalate through two crystallographic porous media of well characterized and highly contrasting geometries: simple cubic (SC) and body centred cubic (BCC). The cyclic fluid strains in the SC cell are symmetric and small (~5). The strains in the BCC cell are even smaller, but there is the potential for non-symmetric flow and there are two contracting regions per unit cell of the lattice. The SC cell is entirely lacking in trailing stagnation points aligned with the flow axis while the BCC contains a trailing stagnation point associated with each sphere within the lattice. Our aim is to aid the understanding of the mechanism of the viscosity increase in porous media flow by giving insight into the importance of the various particular geometries that occur in random porous media.

## Experimental

**Apparatus** The regular porous media flow cells were constructed with 4 mm thick sheet soda glass walls to form square cross-section rectangular boxes to accommodate simple cubic (SC) and body-centred cubic (BCC) arrays of spheres. The cells were packed by hand with soda glass spheres of diameter $d = 5 \pm 0.02$ mm, which were supplied by Sigmund-Lindner of Germany. When packing the SC flow cell some of the spheres had to be glued into position to prevent the array from collapsing during the construction: this was kept to a minimum so as to avoid significant modifications to the porosities of the cells. To pack the BCC array a large number of 5-sphere pyramids were first constructed. Four of the spheres formed four planar corners of a BCC unit cell, with a carefully pre-calculated centre-centre distance, and were fixed in place by being glued to the fifth, body-centred sphere. The five-sphere pyramids were placed into the flow cell such that the four corner spheres formed the first layer of the BCC array. Filling the gaps in the second layer, between the central spheres of the pyramids, ensured that the spacing between all the spheres of the base and second layers was correct. The third and subsequent layers of the array then followed easily.

A schematic diagram of the simple cubic porous media, showing the dimensions of the flow cell, is given in Fig. 1. The body-centred cubic porous media had dimensions 33.9×33.9×195.5 mm to accommodate the larger unit cells of the packing structure. As the number of spheres used to pack the cells, and the dimensions of the spheres and flow cells, were all accurately known, the porosity, $\phi$, of the porous media could be calculated using

$$\phi = 1 - f \tag{2}$$

where $f$ is the packing fraction. The porosity of the SC porous medium was found to be 0.476 and the porosity of the BCC porous medium was found to be 0.32.

The porous media cells were incorporated into the vacuum pump driven flow system shown schematically in Fig. 2. A single-pass vacuum pumping system was used in order give a non-pulsatile flow and to avoid pump degradation of the high molecular weight polymers. The polymer solution (or solvent) was drawn through the test cell from reservoir 1 to reservoir 2 by the vacuum pump. The volume flow rate, U, was controlled by adjusting valves 1 and 2 to control the vacuum pressure inside reservoir 2 and was calculated from a measurement of the pressure drop, $\Delta P_2$, across a calibrated capillary connected to reservoir 1. When an experiment had been completed valve 3 was closed to stop the flow and the vacuum was switched off. The liquid in reservoir 2 could then be either returned to reservoir 1 by opening valve 4, or could be discarded to waste. $\Delta P$ represents the pressure drop measured across the model porous media test cell.

From the measurement of $\Delta P$ as a function of U the resistance coefficient, $\Lambda$, was calculated using

$$\Lambda = \frac{d^2\phi^3(\Delta P/L)}{\eta v(1-\phi)^2} \tag{3}$$

where L is the length of the porous media, $\eta$ is the fluid viscosity and v is the superficial flow velocity (defined by U/cross-sectional-area of porous media).

The Reynolds number for porous media flow is defined as

$$Re = \frac{\rho v d}{\eta(1-\phi)} \tag{4}$$

where $\rho$ is the fluid density. The Ergun equation then states that for Newtonian fluids

$$\Lambda = A + B.Re \tag{5}$$

For low values of $Re$ ($Re < 1$) the resistance coefficient is dominated by the constant term, A. This is the Darcian flow regime in which the pressure drop increases linearly with the flow rate. At higher Reynolds numbers inertial effects become important and the $B.Re$ term in Eq. (5) becomes appreciable. The values of A and B for

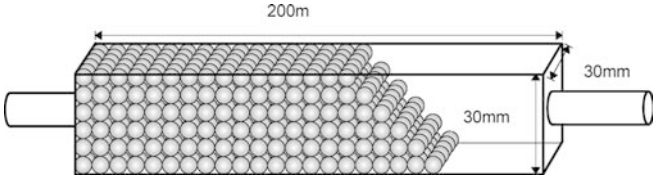


**Fig. 1** Schematic diagram of a crystallographic porous media flow cell, showing the dimensions of the simple cubic porous media

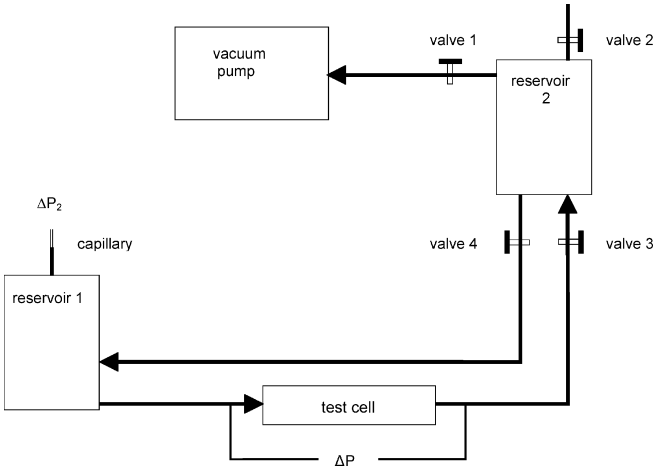


**Fig. 2** Schematic diagram of the vacuum-pump driven flow system used to measure the pressure drop across the porous media as a function of the flow rate

Newtonian liquids are found to vary in the literature. McDonald et al. (1979) suggested values of 180 and 1.8 respectively, after extensive analysis of published data, although both $A$ and $B$ are found to vary within around $\pm 15\%$ due to the precise nature of the packing and the roughness of the particles. According to the numerical computations of Zick and Homsy (1982) the values of $A$ should be approximately 157 and 141 for the simple cubic and body centred cubic porous media, respectively.

Due to differences in the Newtonian values of $A$ and $B$ for the SC and BCC flow cells, estimates of the specific viscosities of polymer solutions were found to allow a more ready comparison between the behaviour in the cells. The specific viscosity, $\eta_{sp}$, was estimated according to

$$\eta_{sp} = \frac{\Lambda_{solution} - \Lambda_{solvent}}{\Lambda_{solvent}} \tag{6}$$

where $\Lambda_{solution}$ and $\Lambda_{solvent}$ represent the polymer solution and the Newtonian values of the resistance coefficient, respectively. Thus, only deviations from Newtonian behaviour appear in the specific viscosity and the pressure drop data from the two porous arrays can be compared for a given polymer solution.

The specific viscosity was plotted as a function of the superficial Deborah number, $De_{\sup}$, defined for porous media flow by Marshall and Metzner (1967) as

$$De_{\sup} = \tau \cdot \frac{v}{d\phi} \tag{7}$$

where $\tau$ is the Zimm relaxation time of the polymer molecule, discussed below. This definition of the superficial Deborah number implies that the superficial strain rate through the porous media would be given by

$$\dot{\varepsilon}_{\sup} = \frac{v}{d\phi} \tag{8}$$

The regular arrays of spheres in the flow cells, the positions of spheres within the SC and BCC unit cells, and the orientation of the flow axis along the symmetry axis of the arrays mean that the two flow cells have distinct characteristics. In the simple cubic flow cell there are no trailing stagnation points in the flow field because every sphere occupies the position of the trailing stagnation point of the previous sphere. In the body-centred cubic porous medium, on the other hand, every sphere possesses leading and trailing stagnation points that are accessible to the flow field. This is because the presence of the body-centred sphere causes a gap between the spheres at the corners of the BCC unit cell. The considerations outlined above indicate that very different extensional flow behaviour may be expected in the two cells.

The two flow geometries both possess repeated expansions and contractions in cross-sectional area, which can produce cyclic transient extensional flow. Using the known geometry of the flow cells, the cross-sectional area of the pore-space, $A$, was calculated as a function of position through each cell. This value was divided by the average cross-sectional area of the pore-space, $\bar{A}$ ($=\phi\times$total cross-sectional area of porous media), to obtain a dimensionless value. Since the flow velocity at any point in the cell must be inversely proportional to A the dimensionless flow velocity is given by $\bar{v} = \bar{A}/A$. From the dimensionless flow velocity dimensionless values for the rate of shear and extensional strain due to variations in the pore-space can be estimated.

Assuming a Poiseuille type flow between the surfaces of adjacent spheres the dimensionless shear rate is given, to a first order approximation, by $\bar{v}/r$, where r is half the distance between the adjacent surfaces. The average value of r at any point in the porous media can be estimated from the value of the cross-sectional area of the voids at that point. The formula used to estimate a dimensionless value for $r$ is given by

$$r \approx \frac{1}{2}\sqrt{\frac{(A/\bar{A})}{n}} \tag{9}$$

where $n$ is the number of spheres that occupy the cross-section of the porous medium at the point of interest.

The dimensionless rate of extensional strain in the porous media due to the variation in the cross-sectional area of the pore space is given by the derivative of $\bar{v}$ with respect to position.

Figures 3 and 4 show the average shear strain rate and the average extensional strain rate, respectively, as a function of position in both the SC and the BCC flow cells. In both cells the local extension rate can be much greater than the superficial rate (based upon the superficial velocity), which has a dimensionless value of 1 (Eq. 8). The figures indicate that both the shear and extensional strain rate may be greater in the pores of the SC cell than the BCC cell due to the more dramatic changes in the cross-sectional area of the pore-space. However the rotation introduced by simple shear components in the flow will hinder the accumulation of molecular strain due to the extensional components so the combined interpretation of Figs. 3 and 4 is extremely complicated. Normally the shear thinning effects associated with the complex simple shear flows illustrated in Fig. 3 would lead to obfuscation of dilatant extensional effects. In the present study we use highly dilute well-characterised solutions in viscous solvents (Boger fluids), substantially removing the variation in the simple shear contribution to the flow resistance.

**Polymer solutions** Dilute solutions of mono-disperse atactic poly(styrene) in di-octyl phthalate (a-PS in DOP) were employed in the experiments. DOP is a viscous, low molecular weight, solvent of viscosity $\eta_{DOP} = 0.04$ Pa.s (Durrans 1971). The $\theta$-temperature for the a-PS/DOP system is 22 °C (Berry 1967).

Three a-PS samples of molecular weights $M_w = 6.9\times10^6$, $M_w = 8.5\times10^6$ and $M_w = 10.2\times10^6$ were used in the experiments. The samples, all supplied by Polymer Laboratories, were closely

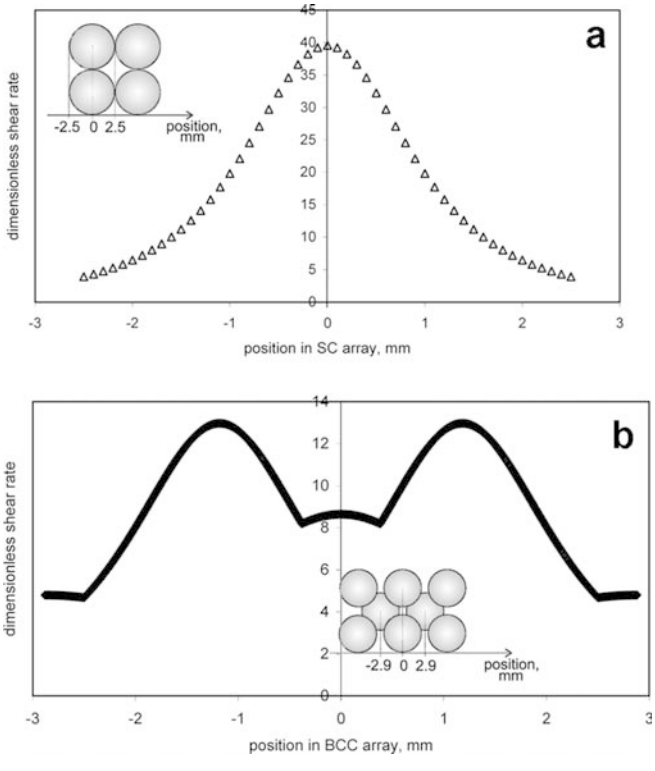


**Fig. 3a,b** Average dimensionless shear rate in the pores, as a function of position through: **a** simple cubic porous media; **b** body centred cubic porous media

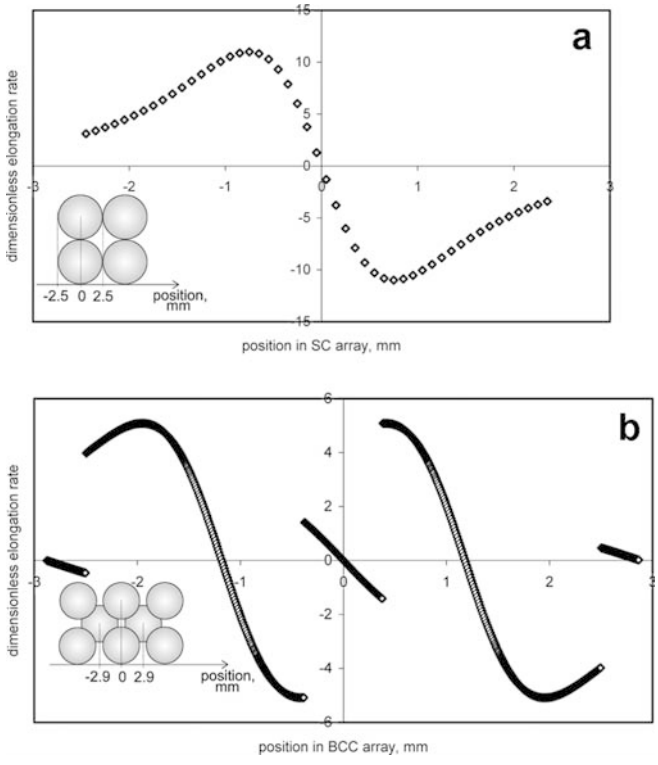


**Fig. 4a,b** Average dimensionless strain rate in the pores, as a function of position through: **a** simple cubic porous media; **b** body centred cubic porous media

monodisperse, having polydispersity indices, $M_w/M_n$, of 1.15, 1.2 and 1.17, respectively. Solutions were prepared in concentrations between 0.005 wt% and 0.03 wt%. These solutions were identical to those used previously to study the flow around single and double spheres (Haward and Odell 2003). The solution temperatures were measured prior to experiment to be $22 \pm 1$ °C.

An estimate of $\tau$ for the polymer solutions was determined from experiments on 0.01% solutions of a-PS in DOP using a new technique called ''oscillatory extensional rheometry'', in which a small volume of fluid is repeatedly oscillated through the stagnation point of a cross-slot device (Odell and Carrington 2001). The molecular weights tested were $M_w = 6.9\times10^6$ and $M_w = 10.2\times10^6$ and the solutions were, in fact, identical to those studied here. The intensity of birefringence was measured as a function of strain rate in the oscillatory cross-slots and the critical strain rate, $\dot{\epsilon}_c = 1/\tau$, of each solution was determined from the points of inflection on the birefringence vs strain rate curves. Such experiments are thought to give reliable estimates of the Zimm relaxation time

$\tau$, including hydrodynamic interactions. The estimates of $\tau$ for the a-PS solutions, including a linear extrapolation for the $M_w = 8.5\times10^6$ sample, are shown in Table 1, together with calculated values for the Zimm relaxation time, intrinsic viscosities calculated from the Mark-Houwink equation and values of $c^*$.

Our estimate of $c^*$ concentration was made on the assumption of each molecule occupying the volume of a cube of dimension $2R_g$, i.e.

$$c^* = \frac{M_w}{N_A(2R_g)^3} \tag{10}$$

where $R_g$ represents the equilibrium radius of gyration and $N_A$ is Avogadro's number. This assumption yields a considerably lower estimate of c* than the common assumption of each molecule occupying a sphere of radius $R_g$, (e.g. Graessley 1980).

From our conservative estimates of c* given in Table 1 it can be seen that our experimental concentrations lie in the range $c^*/42 < c < c^*/7$. For all but our highest experimental concentrations, $c < c^*/10$. For this reason we consider our test solutions to be highly dilute.

From the values of $[\eta]$ given in Table 1, calculated from the Mark-Houwink coefficients for a-PS in DOP, it can be shown that the relative viscosities of our test solutions lie in the range $1.01 < \eta_{rel} < 1.08$. This indicates that our solutions should not be greatly affected by shear flow and could be expected to behave as non-shear thinning Boger fluids.

*Wall effects* Wall effects are an unavoidable complication associated with any flow experiment of this kind, as it is impossible to construct infinite test cells. Packing of the test cells with crystallographic arrays was extremely difficult even with the limited size of the apparatus. However, it should be noted that the ratio of flow cell to sphere dimension in the present experiment is larger than in various related articles, notably Saez et al. (1994) and Haas and Durst (1982), the cross-section of whose porous media comprised a single regular unit cell. If we are to perform and learn from such experiments, wall effects have to be accepted though, of course, minimised wherever possible. Assuming a Poisseuille type flow distribution across the flow cell it is clear that the flow velocity (and therefore *De*) at the flow cell walls will be low in comparison to the core region of the flow cell. Hence extensional flow effects should not dominate the behaviour at the walls. More likely to dominate the flow behaviour at the walls, and other surfaces, is simple shear, the effects of which should be minimised in our experiments by the use of what are effectively Boger fluids. These considerations indicate that flow effects observed in our test cells should not be dominated by the walls of the test cells.

## Results

Figure 5a shows the resistance coefficient as a function of Reynolds number for pure DOP and a 0.02% solution of $M_w = 6.9\times10^6$ a-PS in DOP in the regularly packed porous media. The data points for DOP in both the SC and the BCC porous media obey the Ergun equation (Eq. 5). The BCC porous medium has Ergun coefficients of $A \sim 203$ and $B \sim 6$, reasonably close to the values suggested by McDonald et al. (1979) and Zick and Homsy (1982). The Ergun coefficients for the SC porous medium, on the other hand, are significantly

**Table 1** Estimated Zimm relaxation times, theoretical values for the intrinsic viscosities and c* for a-PS/DOP solutions

| a-PS molecular weight | $6.9\times10^6$ | $8.5\times10^6$ | $10.2\times10^6$ |
|---|---|---|---|
| Experimental relaxation time, $\tau$ (ms) | 2.00 | 2.75 | 3.60 |
| Calculated Zimm relaxation time (ms) | 1.08 | 1.49 | 1.95 |
| $[\eta]$ (Mark-Houwink), $cm^3g^{-1}$ | 210.1 | 233.2 | 255.5 |
| $c^*$(wt%) | 0.26 | 0.23 | 0.21 |

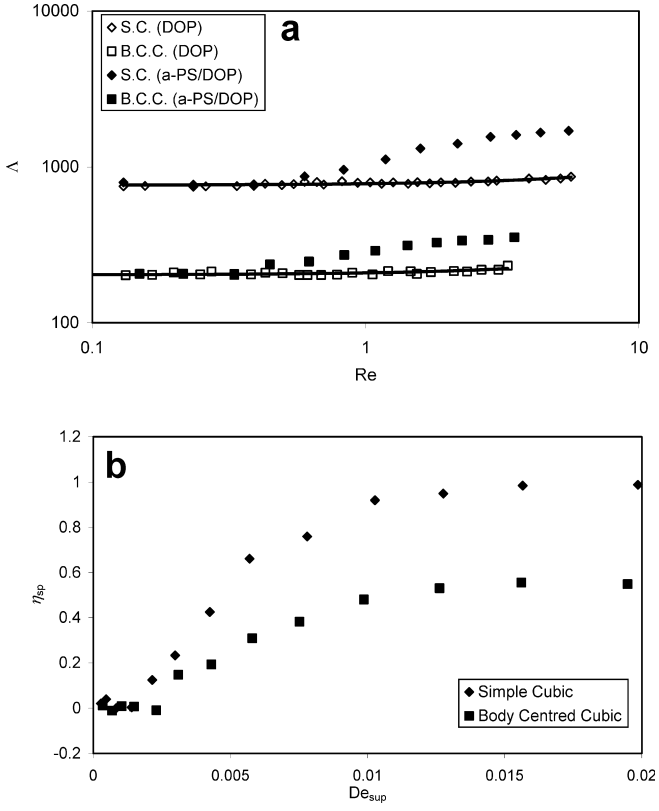


**Fig. 5 a** Resistance coefficient as a function of *Re* in the simple cubic and body centred cubic porous media flow cells for pure DOP and for a 0.02% solution of $M_w = 6.9\times10^6$ a-PS in DOP. **b** Specific viscosity as a function of $De_{sup}$, derived from the data of a

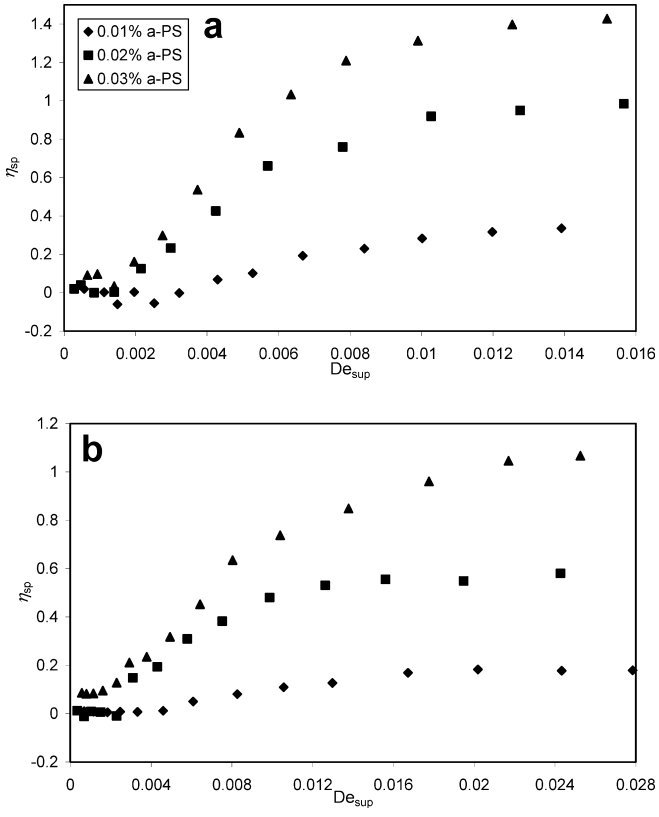


**Fig. 6a,b** Specific viscosity as a function of $De_{sup}$ for solutions of $M_w = 6.9\times10^6$ a-PS in DOP in: **a** simple cubic porous media; **b** body centred cubic porous media

higher than expected ($A \sim 764$, $B \sim 17$). We believe that this is due to a non-uniform flow distribution through the SC array caused by the high porosity and uninterrupted channels in the direction of flow, i.e. the flow may be concentrated along the flow cell axis, which would drive the resistance coefficient up. Hass and Durst (1982) report similar variations in the flow resistance between SC and orthorhombic cells.

The resistance coefficients displayed by the 0.02% solution of $M_w = 6.9\times10^6$ a-PS in DOP in Fig. 5a are typical of those observed in porous media flow of flexible polymers see e.g. Kulicke and Haas (1984) and Saez et al. (1994). The polymer solution shows "pseudo-Newtonian" behaviour at low *Re* but above a critical Reynolds number there is a non-Newtonian increase in the resistance coefficient.

In order to compare the polymer curves in Fig. 5a with each other, Fig. 5b shows the specific viscosity, $\eta_{sp}$, of the fluid in each flow cell as a function of the superficial Deborah number, $De_{sup}$, based upon the Zimm relaxation time; see Experimental section above. It is clear from Fig. 5b that Eq. (7) yields extremely low values for the Deborah number in the context of the coil↔stretch transition theory. The Deborah number for the viscosity increase in Fig. 5b is a factor of ~100 lower than the critical Deborah number for polymer extension (~0.5) predicted by Hinch (1977). However, there is clearly an uncertainty associated with the definition of the Deborah number inside a porous medium because the strain rate will depend upon the position inside the porous matrix. For a given superficial flow velocity there may be positions in the porous matrix where the Deborah number is considerably higher than the value returned by Eq. (7).

A surprising result shown in Fig. 5b is that the specific viscosity in the SC cell rises to a significantly higher plateau value than in the BCC cell. Since the SC cell contains no trailing stagnation points but the BCC cell contains numerous trailing stagnation points this result is contrary to prior expectations based upon the work of Dyakonova et al. (1996) and Haward and Odell (2003).

Figure 6a,b shows the specific viscosity as a function of $De_{sup}$ for solutions of various concentration of $M_w = 6.9\times10^6$ a-PS in DOP in the SC and the BCC flow cells, respectively. As the polymer concentration increases, the plateau in specific viscosity increases approximately proportionally in both porous media

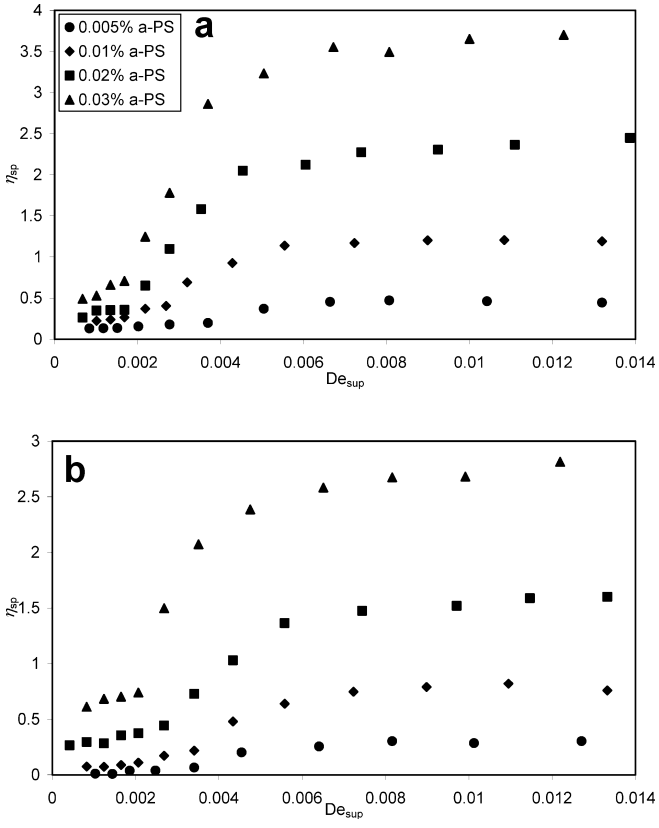


**Fig. 7a,b** Specific viscosity as a function of $De_{sup}$ for solutions of $M_w = 10.2\times10^6$ a-PS in DOP in: **a** simple cubic porous media; **b** body centred cubic porous media

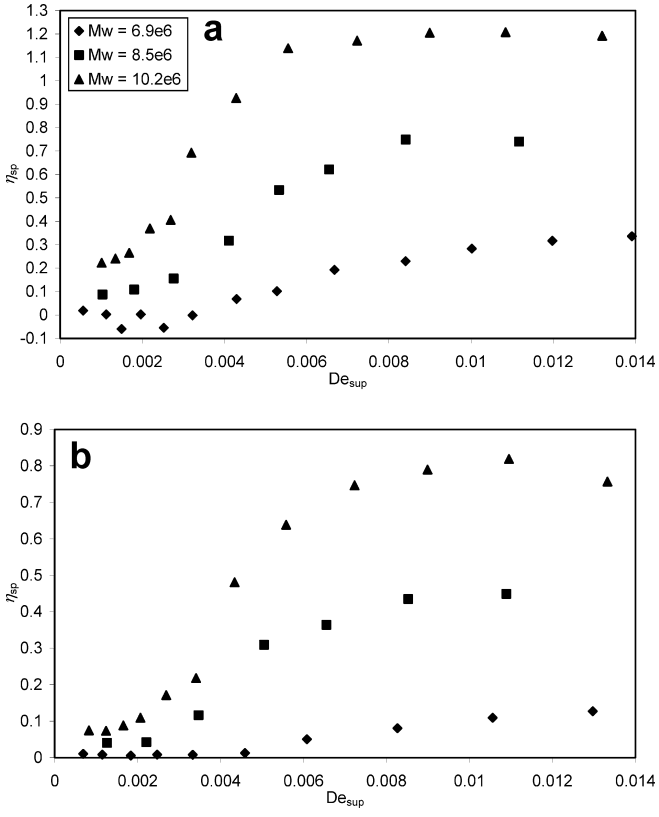


**Fig. 8a,b** Specific viscosity as a function of $De_{sup}$ for 0.01% solutions of a-PS of various molecular weights in DOP in: **a** simple cubic porous media; **b** body centred cubic porous media

cells. For any given polymer concentration the plateau in specific viscosity is significantly higher in the simple cubic than in the body centred cubic, as also observed in Fig. 5b.

Figure 7a,b shows the specific viscosity as a function of $De_{sup}$ for solutions of $M_w = 10.2\times10^6$ a-PS in DOP in the SC and the BCC flow cells, respectively. Non-Newtonian effects which, within experimental uncertainty, scale with concentration are observed at concentrations as low as 0.005%, or $\sim c^*/40$. As before, the critical values of $De_{sup}$ are similar in both flow cells and the specific viscosity consistently reaches higher plateau values in the SC porous media.

Figure 8a,b shows a comparison between different molecular weight polymer samples at 0.01% concentration in the SC and BCC arrays, respectively. As the polymer molecular weight increases the solutions behave more-or-less as expected. For a given polymer concentration the value of $\eta_{sp}$ generally increases with $M_w$ in both the low and high $De_{sup}$ regimes.

The similarities and differences between the behaviour observed in the two regular arrays remain consistent over the entire range of a-PS concentration and molecular weight studied. Although the viscosity increase occurs at a similar superficial Deborah number in both flow cells, and the general behaviour is similar, a higher value of specific viscosity is consistently recorded in the SC cell. This suggests that a-PS molecules generally accumulate a greater strain in the SC array than in the BCC array, or that a greater proportion of molecules become stretched.

## Discussion

The high dilutions of the solutions ($c \ll c^*$ in all cases) and the approximate proportionality of viscosity effects with concentration suggest that the formation of entanglement networks is unlikely. We believe that the viscosification mechanism in the porous media is due to the coil↔stretch transition as envisaged by de Gennes (1974) and Hinch (1977) and observed experimentally in idealised stagnation point extensional flows (Miles and Keller 1980; Keller and Odell 1985).

It was surprising to find that the dilute a-PS/DOP solutions could achieve considerably higher values of specific viscosity in the simple cubic porous medium than in the body centred cubic porous medium. The

expectation prior to the experiment was that the trailing stagnation points in the BCC flow cell would contribute greatly to the accumulation of polymer strain in the cell, while the lack of trailing stagnation points in the SC cell would mean that polymer stretching would be limited. The fact that the apparent extensional viscosity reached higher values in the SC array than in the BCC array may be an indication that a strong transient extensional flow field can arise in the varying cross-section pore-space of the SC array, despite the absence of trailing stagnation points in the flow cell.

For the flow of a-PS/DOP solutions around two axially aligned spheres it has been shown that highly viscous oriented strands of polymer emanating from the trailing stagnation point of the leading sphere may screen the flow around the trailing sphere (Haward and Odell 2003). This leads to a reduction in viscous force experienced by the trailing sphere, relative to the leading sphere, and a corresponding reduction in the level of birefringence, i.e. molecular strain, in the wake of the trailing sphere. If this result can be extrapolated to a third or fourth sphere in line it can be imagined that the viscous force and molecular strain could be further reduced with successive spheres.

In the BCC porous medium every sphere in the array is situated directly downstream of the trailing stagnation point of the preceding sphere. It can therefore be seen that many of the trailing stagnation points in the BCC array may be screened from the flow field by viscous oriented strands emanating from the trailing stagnation points of previous spheres and, therefore, may not play a significant role in increasing the extensional viscosity. It can now be pictured that the extended macromolecules that are screening the trailing stagnation points must be travelling through the pores of the array. As such the fluid situated between successive aligned spheres may effectively be stagnant so the variation in cross sectional area of the pores could become the most important component in the extensional flow field.

It seems that the manner in which spheres pack tightly together may, in one way or another, effectively remove the trailing stagnation points from the flow field. In the simple cubic structure the spheres themselves obstruct the trailing stagnation points. In the body centred cubic the stagnation points are screened in a similar way to that observed in flow around two aligned spheres (Haward and Odell 2003). Porous media modelled by randomly packed beds of spheres will mainly consist of very close packed structures (face-centred and hexagonally close packed unit cells). Dislocations may, at most, result in sporadic occurrences of simple cubic and body centred cubic unit cells. This may be an explanation for the result of Haas and Durst (1982) who found the specific resistance coefficient of a randomly packed bed of spheres could be calculated by a linear superposition of the specific resistance coefficients of two regularly packed beds of spheres, neither of which contained trailing stagnation points.

Real porous media in sedimentary layers may well present effective stagnation points at bifurcations and pore entrances and, in this respect, may not be well modelled by closely packed beds of spheres or ballotini.

Another surprising result from this study was the low value of apparent Deborah number at which the non-Newtonian viscosity increases occurred in the a-PS/DOP solutions. Although it may appear that the results obtained from the a-PS solutions in the regular arrays do not fully obey the coil↔stretch transition theory it should be mentioned again that the definition of $De_{\mathrm{sup}}$ in porous media (Eq. 7) is uncertain due to the complex geometry of the flow field.

Since stagnation points do not seem to play the major role in the flow fields of our crystallographic porous media we propose that modifications should be made to Eq. (7) for $De_{\mathrm{sup}}$. Following the method of Haas and Durst (1982), Fig. 4 shows the local extensional strain rate in the pores of the porous media may increase the local Deborah number by around an order of magnitude over the value returned by Eq. (7). However, this still leaves the apparent Deborah number based on the Zimm relaxation time $\sim$0.05, about one-tenth of the expected value.

Since DOP at room temperature is a theta solvent for a-PS, the a-PS molecule is expected to have a non-free draining conformation at equilibrium. Upon stretching the molecule is therefore expected to increase its relaxation time from $\tau_{Zimm}$ to $\tau_{Rouse}$ (or more properly the Zimm relaxation time in the absence of hydrodynamic interactions within the coil). The increase in the molecular relaxation time is expected to cause hysteresis in the coil↔stretch transition, as predicted by de Gennes (1974).

As explained in the Background section, dumbbell simulations do not generally show accumulation of strain in time-symmetrical extensional flows, even with de Gennes type hysteresis incorporated. Dyakonova et al. (1996) speculate on mechanisms that can break the symmetry, even at low Reynolds number. However, recent simulations by Odell and Carrington (2001) using the Chilcott-Rallison FENE dumbbell model (Chilcott and Rallinson 1988) have shown that molecules exhibiting coil↔stretch hysteresis may be able to accumulate strain under such conditions without the need for an asymmetric flow field, but only for a modest range of $De > 0.5$ and strongly dependent upon the initial start-up conditions.

In the BCC porous medium, periodic variations in the total cross-sectional area of the pore-space are clearly equal and opposite. However, expansions and contractions from pore to pore are not necessarily symmetrical since, following each contraction, a streamline or fluid element has a choice of pores into

which the flow can expand, and vice-versa. In the SC porous medium, on the other hand, flow from pore to pore probably does result in periodic equal and opposite contractions and extensions of fluid elements. In any case it seems evident that polymers can stretch in the pore-space of the regular porous media since large increases in the specific viscosity have been observed in the SC porous media, which is time-symmetric and in which there are no trailing stagnation points present.

One possible explanation for the apparent molecular extension at low values of $De_{\mathrm{sup}}$ is that Poiseuille-like flow between adjacent spheres significantly increases the local strain rate, although we believe this may only account for a factor of $\sim 2$.

A second possibility is that in porous media flows non-equilibrium molecular conformations (or the appearance of pre-stretched polymer molecules) are important; see, e.g. Perkins et al. (1997). If a pre-stretched polymer molecule presents itself at a pore entrance the appropriate Deborah number should be based upon the relaxation time without hydrodynamic interactions ($\tau_{Rouse}$), which is considerably greater than the Zimm relaxation time with which our experimental Deborah numbers are calculated. An important difference between flow around spheres and idealized extensional flows with stagnation points compared with porous media flows is that, in cyclic contracting flows such as porous media, molecules have many opportunities to explore non-equilibrium conformations at pore entrances. The sporadic occurrence of pre-stretched molecules would also serve to reduce the strain required to achieve a high degree of stretching. Once extension of molecules begins it becomes a runaway process resulting in highly strained molecules. This could explain the effective molecular extension at low Deborah number in porous media and has significant relevance to enhanced oil recovery applications.

Assuming that the a-PS molecules can accumulate strain due to the varying cross sectional area of the pore-space in the porous media, and that the trailing stagnation points in the BCC cell are effectively screened from the flow field, then Fig. 4 shows that the extensional strain rate in the pores of the SC cell may in fact reach a significantly greater periodic maximum than in the BCC cell. Therefore, for a given superficial flow velocity, it may be expected that a greater percentage of the molecular weight distribution could become stretched in the SC cell than in the BCC cell, possibly accounting for the differences in the plateau values of specific viscosity observed in the two cells.

The observed magnitude of extension thickening would depend upon both the degree of molecular stretching and the proportion of molecules undergoing high strains. Stagnation points certainly yield high strains, but typically as narrow strands of stretched material involving only a small proportion of the whole solution. Contraction stretching in the pores, on the other hand, may yield lower molecular strains, but involves the whole solution.

## Conclusions

We have examined dilute solutions of monodisperse atactic poly(styrene) in DOP in two regularly packed porous beds: body centred cubic which contains trailing stagnation points and simple cubic which is devoid of trailing stagnation points. By measuring the pressure difference across the porous beds as a function of the flow velocity we have been able to estimate the non-Newtonian increases in specific viscosity as a function of the superficial Deborah number.

Contrary to expectations, a greater increase in specific viscosity was observed in the simple cubic array than in the body centred cubic array. We explain this result as being due to a greater periodic extensional strain rate through the pores of the simple cubic array and also to the possibility that the trailing stagnation points in the body centred cubic array may be screened from the flow field by strands of extended polymer. The a-PS molecules may be able to accumulate strain in the transient periodic extensional flow field in the pores of the arrays as DOP is a theta solvent for a-PS and therefore hysteresis is to be expected in the coil↔stretch, extension/relaxation process. This may occur at low $De$ due to the presence of pre-stretched, non-equilibrium, molecular conformations being present at pore entrances and having the Rouse relaxation time.

Considering the high dilution of the solutions used in the study, we see no reason to attribute the increase in flow resistance to anything other than an increase in extensional viscosity of the solutions due to the coil↔stretch transition.

**Acknowledgements** We gratefully acknowledge the support of the EPSRC and the EU Alfa programme.

## References


Berry GC (1967) Thermodynamic and conformational properties of polystyrene. II. Intrinsic viscosity studies on dilute solutions of linear polystyrene. J Chem Phys 46:1338–1352

Chilcott MD, Rallison JM (1988) Creeping flow of dilute polymer solutions past cylinders and spheres. J Non-Newtonian Fluid Mech 29:381–432

Cogswell FN (1978) Converging flow and stretching flow: a compilation. J Non-Newtonian Fluid Mech 4:23–38

Cressely R, Hocquart R (1981) Extension and relaxation of high macromolecules in oscillatory elongational flow using flow birefringence. Polym Prepr 22:120–121

Dauben DL, Menzie DE (1967) Flow of polymer solutions through porous media. J Pet Technol 19:1065–1073

de Gennes PG (1974) Coil-stretch transition of dilute flexible polymers under ultrahigh velocity gradients. J Chem Phys 60:5030–5042

Durrans TH (1971) Solvents, 8th edn. Chapman and Hall, London

Durst F, Haas R, Kaczmar BU (1981) Flows of dilute hydrolyzed polyacrylamide solutions in porous media under various solvent conditions. J Appl Polym Sci 26:3125–3149

Dyakonova NE, Odell JA, Brestkin YV, Lyulin AV, Saez AE (1996) Macromolecular strain in periodic models of porous media flows. J Non-Newtonian Fluid Mech 67:285–310

Graessley WW (1980) Polymer chain dimensions and the dependence of viscoelastic properties on concentration, molecular weight and solvent power. Polymer 21:258–262

Haas R, Durst F (1982) Viscoelastic flow of dilute polymer solutions in regularly packed beds. Rheol Acta 21:566–571

Haward SJ, Odell JA (2003) Molecular orientation in non-Newtonian flow of dilute polymer solutions around spheres. Rheol Acta (submitted)

Hinch EJ (1977) Mechanical models of dilute polymer solutions in strong flows. Phys Fluids 20:S22–S30

James DF, McLaren DR (1975) The laminar flow of dilute polymer solutions through porous media. J Fluid Mech 70:733–752

James DF, Saringer JH (1980) Extensional flow of dilute polymer solutions. J Fluid Mech 97:655–672

Keller A, Odell JA (1985) The extensibility of macromolecules in solution: a new focus for macromolecular science. Colloid Polym Sci 263:181–201

Kulicke WM, Haas R (1984) Flow behaviour of dilute polyacrylamide solutions through porous media. 1. Influence of chain length, concentration, and thermodynamic quality of the solvent. Ind Eng Chem Fundam 23:308–315

Marshall RJ, Metzner AB (1967) Flow of viscoelastic fluids through porous media. Ind Eng Chem Fundam 6:393–400

McDonald IG, El-Sayed MS, Mow K, Dullien FAL (1979) Flow through porous media—the ergun equation revised. Ind Eng Chem Fundam 18:199–205

Miles MJ, Keller A (1980) Conformational relaxation time in polymer solutions by elongational flow experiments. 2. Preliminaries of further developments: chain retraction; identification of molecular weight fractions in a mixture. Polymer 21:1295–1298

Muller AJ, Saez AE (1999) In: Nguyen TQ, Kausch HH (eds) Flexible chain dynamics in elongational flows: theory and experiment. Springer, Berlin Heidelberg New York

Muller M, Vorwerk J, Brunn PO (1998) Optical studies of local flow behaviour of a non-Newtonian fluid inside a porous medium. Rheol Acta 37:189–194

Odell JA, Carrington SP (2001) Extensional flow oscillatory opto-rheometry. Presented at Physical Aspects of Polymer Science, Cambridge, UK

Odell JA, Muller AJ, Keller A (1988) Non-Newtonian behaviour of hydrolysed polyacrylamide in strong elongational flows: a transient network approach. Polymer 29:1179–1190

Perkins TT, Smith DE, Chu S (1997) Single polymer dynamics in an elongational flow. Science 276:2016–2021

Saez AE, Muller AJ, Odell JA (1994) Flow of monodisperse polystyrene solutions through porous media. Colloid Polym Sci 272:1224–1233

Zick AA, Homsy GM (1982) Stokes flow through periodic arrays of spheres. J Fluid Mech 115:13–26